Microchemical Journal 206 (2024) 111511

Contents lists available at ScienceDirect

Microchemical Journal

journal homepage: www.elsevier.com/locate/microc

Sorption experiments as efficient as possible: Mini-column experiments (MCE) using HPLC-ICP-MS coupling with a new data analysis approach to determine sorption parameters

Aaron Haben *, Kristina Brix, Nico Bachmann, Ralf Kautenburger

WASTe Group, Inorganic Chemistry, Saarland University, Saarbrücken, Germany

ARTICLE INFO

Keywords:
HPLC-ICP-MS-coupling
Mini-column
Sorption
Cs(I)
Eu(III)

ABSTRACT

To quantify retention and sorption parameters, diffusion-, batch- or column experiments are common practice. However, these are either not close to nature, extremely time-consuming or material intensive. A promising approach to eliminate these problems is the performance of mini-column experiments (MCE). Due to dynamic retention and realistic solid–liquid ratios, these are close to nature and resource-efficient. The aim of this work is to perform highly controllable MCE using a HPLC (high-performance liquid chromatography) system and HPLC-ICP-MS (inductively coupled plasma mass spectrometry) coupling. With this approach, ultra-fast sorption experiments are possible only using 100–150 mg adsorbent and 160 mL eluent. That means, sorption experiments are even more time- and cost-efficient and also more controllable than with conventional methods. The presented method is based on a newly developed MCE-HPLC-ICP-MS coupling, which was applied to investigate the sorption of Eu(III) on kaolinite and sand in 10 mM NaCl. With that it was possible to carry out dynamic sorption experiments in just 5–15 h and thus determine e.g. maximum loading capacity (q_{max}) in a very short amount of time. Furthermore, a quantification method for eluates of high ionic strength is presented. Here, the sorption of Cs(I) on calcium silicate hydrate (C-S-H) phases in 10 mM and 100 mM NaCl was investigated. For validation, the sorption distribution ratios (R_d) obtained were compared with those from batch experiments. These agreed very well with each other and with those from the literature. Overall, with MCE more sorption parameters can be determined much faster, more accurately and more efficient than with the conventional methods.

1. Introduction

To investigate the retention behaviour of different substances on multiple adsorption materials, the most common method used are batch sorption experiments. Here one or multiple test series with a set of many individual samples are investigated under precisely defined conditions. This enables the determination of simple sorption parameters, like distribution coefficients (K_d values) as a function of the test parameters used [1–6]. However, batch experiments are, due to the unrealistic solid–liquid ratios and static equilibrium, not as close to nature as other experimental setups. Two other (common) methods to investigate or determine retention parameters are diffusion and column experiments. These are predominantly close to nature but are also either very time-consuming and/or material intensive [7,8].

A few years ago, initial attempts were made to develop a more efficient and realistic method for carrying out sorption experiments. The idea was to fill real mini-columns with adsorbent material and carry out mini column experiments (MCE) using high-performance liquid chromatography (HPLC) devices [8–10]. With such an experimental setup, in theory only 50–300 mg of adsorbent and less than 300 mL of eluent are required. But, until now, there has been no valid MCE method to describe sorption processes or to calculate chemical-physical sorption parameters. In this work we present a new MCE method that can be used to derive dynamic sorption distribution ratios (R_d) and maximum loading capacities (q_{max}) for mono- and higher-valent metal ions on strongly sorbing solid phases. With this method, various adsorbents (calcium silicate hydrate phases, kaolinite and sand) are compacted in mini-columns (100–150 mg) and connected to the HPLC to analyse the retention behaviour of Cs(I) and Eu(III) as strongly sorbent metal ions under precisely defined conditions. Cs(I) was selected as the first analyte to test the MCE method because it is only present as $Cs^{+}_{(aq)}$ over the entire pH range of 2–14 and it does not precipitate under natural conditions

* Corresponding author at: Institute of Inorganic Chemistry – WASTe-Elemental Analysis Group, Campus C4.1, 66123 Saarbrücken, Germany.
E-mail address: aaron.haben@uni-saarland.de (A. Haben).

https://doi.org/10.1016/j.microc.2024.111511
Received 30 April 2024; Received in revised form 22 August 2024; Accepted 23 August 2024
Available online 24 August 2024

[11–13]. This simplifies the investigations at the beginning, as no further retention effects are to be expected apart from adsorption. After optimising the method, the trivalent Eu(III) was also selected, which shows strong retention effects (in addition to sorption and precipitation) and is used in the MCE as a less toxic and non-radioactive homologue for Cm(III) and Am(III) [14–16]. The retention was quantified either via a newly developed HPLC-ICP-MS (inductively coupled plasma mass spectrometry) coupling or by means of a fraction collector and subsequent ICP-MS measurement. Regarding the HPLC-ICP-MS coupling, also a new data evaluation is presented here.

All adsorption materials investigated in this study are components of possible barrier materials for a potential repository for high-level nuclear waste (HLW) in Germany [17]. The most dangerous components of HLW are enriched uranium from the nuclear fuel elements and its fission products, such as Cs(I) or Eu(III), whereas Eu(III) also acts as homologues to Sm(III), Am(III) and Cm(III) [13–16,18]. Due to their chemical and radiotoxic properties, a hypothetical exposure of these radionuclides in the environment would thus have a permanently damaging effect on humans and nature. To effectively protect future generations from the harmful effects of radionuclides, the final storage of HLW in deep geological formations is envisaged [17,19–21].

For Germany a storage in geological host rock formations at depths of 250–1000 m using natural and artificial barriers (multi-barrier system) is planned. This consists of the HLW-containing castor casks, cement-based materials, which are used as construction, closure and/or backfill materials, further backfill in and around the area used for final disposal (most likely clay based materials) and the geological formation in which the waste is emplaced (the host rock) [1,17,19,20]. As a result, the investigation of the retention behaviour of repository-relevant elements or element mixtures under different geochemical conditions in cement-based materials, their alteration products and clay minerals are of great interest. But solutions in equilibrium with hydrated cement are hyperalkaline and the minerals are not thermodynamically stable in contact with penetrating water and tend to corrode over time. This results in cement aging phases, which consist essentially of calcium silicate hydrate (C-S-H) phases and form solutions with pH values between 10 and 13. Since both freshly hydrated and aged cement consist mainly of C–S-H phases and these are considered to be responsible for the heavy metal binding ability of cementitious materials, they are a central component of risk assessment in current repository research and are also investigated in this work [4,22–24]. Another, more stable, adsorbent material used in this study is kaolinite, which is one of the most common clay minerals and the simplest among the aluminosilicate clays [25]. Therefore, kaolinite is ideal as a simple model for clay minerals as a possible geotechnical barrier.

During the MCE, the analytes are injected into the eluent and with that onto the column. After subsequent analysis of the eluate using ICP-MS, the retention behaviour can then be determined and retention parameters calculated. For kaolinite as adsorbent material, direct quantification can be carried out via HPLC-ICP-MS coupling. However, at present, the ionic strength of the eluate is a limiting factor for quantification via HPLC-ICP-MS coupling. Since C-S-H-phases tend to leach in aqueous media, high concentrations of Ca(II) and Si(IV) ions are to be expected and a workaround of the coupling must be investigated in advance [26,27]. For this case of excessive leaching, an alternative method is also presented in this work. Hereby, the eluate is collected by means of a fraction collector and, after subsequent processing, the fractions are also analysed using ICP-MS. In addition, this experimental approach also allows a more detailed investigation of the leaching behaviour itself.

2. Materials and methods

2.1. Chemicals

Ultrapure water (0.055 μS cm^{-2}) (PURELAB® Chorus 1 ultrapure water filtration unit, Elga LabWater, High Wycombe, UK) was used to prepare all solutions. NaCl with premium-grade quality (EMSURE®) from Merck (Darmstadt, Germany) was used to prepare the eluents for MCEs and the electrolytes for the batch experiments. A solution with 10 mg L^{-1} of Sc(III) (1,000 mg L^{-1} in 5 % HNO_3, Alfa®, Karlsruhe, Germany) and Ho(III) (1,000 mg L^{-1} in 2–3 % HNO_3, Merck Certipur®, Darmstadt, Germany) in ultrapure water was prepared as the internal standard stock solution for all ICP-MS measurements. HNO_3 (Rotipuran® Supra 69 %, Carl Roth, Karlsruhe, Germany) was used to acidify the measurement solutions, whereas HCl (HCl 30 % Suprapur®, Merck Supelco®, Darmstadt, Germany) and NaOH (Suprapur® 30 %, Merck, Darmstadt, Germany) were used to adjust the pH in the experiments. Argon 5.0 (Ar ≥ 99.999 mol%, ALPHAGAZ™ 1 Argon, Air Liquide, Düsseldorf, Germany) was used as plasma gas for ICP-MS measurements. For the experiments and ICP-MS calibration, Cs(I) (1,000 mg L^{-1} in 2.5 % HNO_3, AccuStandard, New Haven, USA) and Eu(III) (10,000 mg L^{-1} in diluted HNO_3, Agilent, Kingstown, USA) ICP-MS standard solutions were used. Furthermore, Ca(II) (1,000 mg L^{-1} in 0.5 mol L^{-1} HNO_3, Merck Certipur®, Darmstadt, Germany) and Si(IV) (10,000 mg L^{-1} in water. Tr. HF, AccuStandard, New Haven, USA) standards were used for ICP-MS calibration of the leaching experiments.

The used C-S-H phase is commercially available Circosil® 0.1 from Cirkel (Emsdetten, Germany). Cirkel states for the Circosil® structure that it consists of 88 % tobermorite phases ($5CaO{\cdot}6SiO_2{\cdot}5H_2O$) and 10 % embedded SiO_2. With this information and additional XRF-data (X-ray fluorescence spectroscopy) provided by Cirkel, a molar Calcium to Silicon ratio (C/S) of approx. 0.65 can be calculated. However, if only the tobermorite part is used as a basis for calculation, the C/S ratio would be 0.83 [28,29]. For the MCE with HPLC-ICP-MS coupling a mixture of kaolinite KGa-1b (Georgia, USA), sold by the Clay Minerals Society (Chantilly, USA) and quartz sand (purified sea sand, Merck, Darmstadt, Germany) were used as stationary phases in the column.

2.2. Preparing the mini columns

The mini columns used are HPLC guard columns (UPC-130B, UPCHURCH SCIENTIFIC™, Oak Habor, USA); either in factory condition (2 mm ID) or drilled out to 3.5 mm ID. In addition, two different filter discs were used: one with a pore size of 500 nm (A-103X, UPCHURCH SCIENTIFIC™, Oak Habor, USA) and one with a pore size of 100 nm (Stainless steel filter disc, Applied Research Europe, Berlin, Germany). To guarantee impermeability using the stainless-steel filter disc (SSFD), a strip of parafilm approx. 1–2 mm wide and approx. 70 mm long was wrapped around it before it was installed in the column. To fill the column, it was clamped in a vice, the dry adsorbent was filled into the column with a suitable funnel and thereby gradually compacted.

2.3. MCE without coupling

The HPLC components used are Agilent 1100 and 1200 HPLC systems (Waldbronn, Germany) and listed in Table 1.

The MCE were performed with 10 mM or 100 mM NaCl as eluent and at 25 °C column temperature. For both, the 3.5 mm ID columns were packed with Circosil® (150.1 mg for the experiment with 10 mM NaCl and 152.1 mg for the one with 100 mM NaCl), sealed with the SSFD and then preconditioned in the HPLC for 150 min using a flow gradient from 10 to 40 μL min^{-1}. After preconditioning the flowrate (Q) of the eluent was set to 40 μL min^{-1}. In advance to the experiments the Cs(I) ICP-MS standard solutions were neutralised with NaOH each and used for injection. Therefore, the concentrations of the injection solutions were 948.2 mg/L and 959.0 mg/L for the MCE in 10 mM and 100 mM NaCl. For each experiment 100 times 12.47 μg (in 10 mM NaCl) or 9.48 μg (in 100 mM NaCl) of Cs(I) were injected into the eluent in 38 min intervals (97.8 or 75.3 nmol Cs(I) per injection). Behind the column, the entire eluate was collected by means of a fraction collector. Samples were taken from the individual fractions for an ICP-MS measurement and the

Table 1
Components and software of used HPLC system in MCE without coupling.

Hardware:	
1100 Series G1379A Degasser	
1100 Series G1312A Binary Pump	
1100 Series G1313A ALS	
1100 Series G1316A Colum	
1100 Series G1315B DAD	
1200 Series G1364C Analyte FC	
Software:	
ChemStation for LC 3D Systems Rev. B.02.01-SR2 [260]	

pH values were determined (pH-meter SevenMulti, pH-electrode InLab®, Mettler Toledo, Columbus, USA). For the ICP–MS measurement, an Agilent 8900 ICP-QQQ (Santa Clara, USA) with an Agilent SPS 4 autosampler (Santa Clara, USA) was used. Therefore, 20 µL of the fractions were added to 9.67 mL Milli-Q water, 300 µL HNO_3 (69 %) and 10 µL internal standard stock solution. The measurement was performed with different cell gas modes: ^{28}Si and ^{40}Ca were measured in H_2 mode via mass pair (Q_1, Q_2) = (28, 28) and (Q_1, Q_2) = (40, 40) and ^{133}Cs in "NoGas"-mode. An external calibration was done for quantification.

2.4. Leaching of C-S-H phases

Since C-S-H phases are known for their strong leaching behaviour, it can be assumed that the mass of Circosil® in the column is not constant during one experiment [26,27]. Most of the calculations described in chapter 2.7 require the exact mass of the adsorbent material. This is why leaching studies where performed. Hereby multiple MCE with the 3.5 mm ID column and different experimental conditions were performed (described in Table 2). In all cases, Q was 40 µL min^{-1} and the column temperature was again 25 °C. To simulate Circosil® at a late stage in the experiment, i.e., already leached Circosil®, two of the four samples were treated (washed) in advance. Therefore 24.17 g of Circosil® were weighed out and then suspended 8 times with ultrapure water, stirred and decanted. Afterwards, the suspension was filtered through a suction flask and filter paper with a pore size of 7 µm and washed again 8 times with ultrapure water. The remaining solid was then dried to constant weight (7 days) at 110 °C to give 19.57 g of washed Circosil®. All filled columns were preconditioned using the same flow gradient as described in chapter 2.3.

The eluate was collected in the fraction collector and afterwards the pH values, the Ca(II)- and the Si(IV)-concentration in the fractions were determined. To quantify the leached Ca(II)- and Si(IV)-concentrations, ICP-MS measurements were performed analogue to the MCE described in chapter 2.3.

2.5. Batch experiments

For the batch experiments, 10 mL of either 10 mM or 100 mM NaCl solution was added to 40 ± 0.2 mg Circosil® (S/L=4 g/L) in a 15 mL polypropylene (PP) centrifuge tube (Ultra-High Performance Centrifuge Tube, VWR® International, Darmstadt, Germany), followed by equilibration in a horizontal shaker (Promax 1020 platform shaker, Heidolph Instruments, Schwabach, Germany) at room temperature for 7 days. This resulted in a pH value of 10.7 for all samples (analogue to the MCE, see chapter 3.1 and 3.2). Cs(I) was then added at concentrations of 0, 0.5, 2.5, 10, 50, 250, 1,000, 5,000, 25,000, 50,000 µg/L and then again shaken for 7 d. For better statistical evidence, all samples were prepared in triplicates. Phase separation was carried out in a centrifuge (Centrifuge 3-18KS, Sigma, Osterode am Harz, Germany) at 16,990 g for 30 min at 21 °C. Then 10 µL to 1 mL of the supernatant solution (depending on dilution) was taken and the ICP–MS measurement solutions were prepared analogue to chapter 2.3. Quantification of Cs(I) was performed as described in chapter 2.3.

Table 2
Leaching MCE and their experimental conditions.

MCE	Adsorbent	Filter disk	Eluent	Injection
L 1	Circosil®	A-103x	10 mM NaCl	5 µL ultrapure water
L 2	Circosil® washed	SSFD	100 mM NaCl	5 µL ultrapure water
L 3	Circosil® washed	SSFD	10 mM NaCl	5 µL of 500 mg/L Cs(I)-solution
L 4	Circosil®	A-103x	10 mM NaCl	5 µL of 500 mg/L Cs(I)-solution

2.6. MCE with HPLC-ICP-MS coupling

Here the HPLC components used are Agilent 1260 Infinity II HPLC systems (Waldbronn, Germany) and listed in Table 3.

The HPLC system was coupled to the ICP-MS (Agilent 8900 ICP-QQQ, Santa Clara, USA) via a PEEK capillary (1/16″ x 0,13 mm ID, nature with red stripes, ERC, Riemerling, Germany) and a split-flow-valve (SFV; UP P-451, Flow-Splitter, Upchurch Scientific, Oak Habor, USA). The experimental setup is schematically shown in Fig. 1.

For the experiments the 2 mm ID column was packed with either 102.5 mg sand or 104.4 mg of a 1:9 wt% kaolinite/sand mixture. In this case, the columns were sealed with the A-103x filter disc. The columns were preconditioned with a flow gradient from 10 to 100 µL min^{-1} for 120 min. A 10 mM NaCl solution with a flow rate of 100 µL min^{-1} was used as eluent and a column temperature was again set to 25 °C. The split of the SFV was set to approximately 1:7.5 (13.3 % of the flow goes to the ICP-MS). To increase the flow to the nebuliser, an internal standard solution containing 5 % HNO_3, 1 ppb Sc and 1 ppb Ho was introduced via the Peri Pump (0.2 rps) through a T-piece. During the experiments 5 µL of an Eu(III) solution with a concentration of either 70 mg/L (on sand; 2.30 nmol Eu(III) per injection) or 100 mg L^{-1} (on kaolinite/sand mixture; 3.29 nmol Eu(III) per injection) were injected. The ICP-MS quantification was carried out using a time-resolved (TRA) measurement method.

To provide initial validation of the HPLC-ICP-MS coupling, another MCE was performed with Eu(III) on a kaolinite/sand mixture using the method with fraction collector described in section 2.3. Here 375.3 mg of the 3:7 wt% kaolinite/sand mixture was packed in the 3.5 mm ID column and 5 µL of a 700 mg/L Eu(III) solution (23.0 nmol per injection) was injected multiple times into 10 mM NaCl. Quantification was also performed as described in chapter 2.3.

2.7. Data evaluation of MCE

To quantify the retention behaviour of the analytes the total recovery (R) in % gets calculated as shown in equation (1).

$$R = \frac{C_0}{C_{eq}} \bullet 100\% \quad (1)$$

Table 3
Components and software of used HPLC system in MCE with HPLC-ICP-MS coupling.

Hardware:
1260 Infinity II G7111B Quat Pump
1260 Infinity II G7129A Vialsampler
1260 Infinity II G7116A MCT
1260 Infinity II G7117C DAD HS
Software:
OpenLab CDS ChemStation Edition Rev. C.01.10 [322]

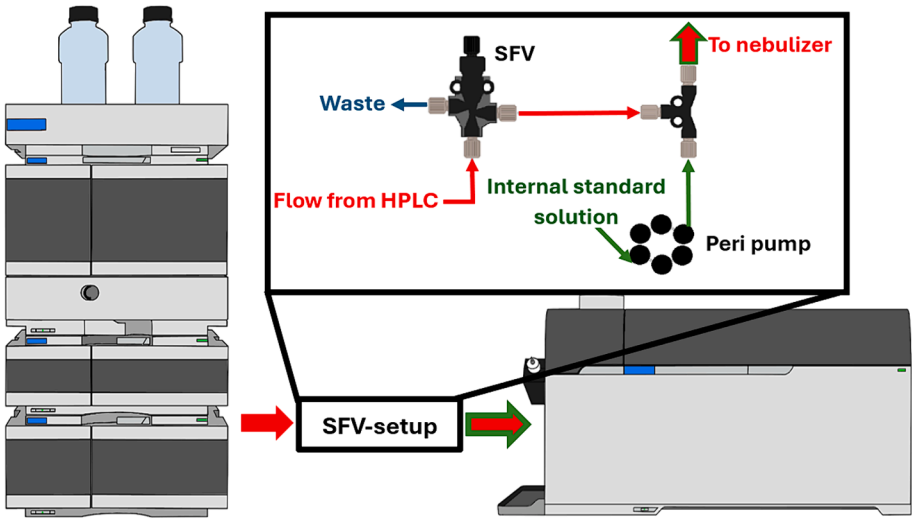

Fig. 1. Schematic diagram of the HPLC-ICP-MS coupling used for the MCE (SFV. split-flow-valve).

Since the MCE analysis performed are injection-based the initial analyte concentration C_0 [mg/L] must be calculated as shown in equation (2), whereas the equilibrium concentration C_{eq} [mg/L] is the not immobilised amount in the liquid phase which is measured via ICP-MS.

$$C_0 = \frac{C_{in} \bullet V_{in}}{Q \bullet t} \tag{2}$$

In equation (2) C_{in} [mg/L] is the concentration of the injection solution, V_{in} [mL] the injection volume, Q [mL min^{-1}] the flowrate of the eluent and t [min] the time between each injection.

An other widely used method to quantify the retention is to calculate the sorption distribution ratio R_d [L kg^{-1}] (or $\log(R_d)$) shown in equation (3). The parameter q [mg g^{-1}] (in equation (3) [mg kg^{-1}]) is the loading of the analyte onto the adsorbent.

$$R_d = \frac{q}{C_{eq}} \tag{3}$$

Especially in the context of the MCE, where a large amount of data, like break through curves (BTC), are generated, the possibility to fit the experimental data with model calculations is particularly interesting. Two of the simplest sorption models are the Freundlich (equation (4)) and Langmuir (equation (5)) isotherms. Here K_F [L g^{-1}] is the Freundlich coefficient, n the Freundlich exponent, K_L [L g^{-1}] die Langmuir coefficient and q_{max} [mg g^{-1}] the maximal loading capacity of the analyte onto the adsorbent. The Freundlich isotherm assumes multilayer adsorption on heterogeneous surfaces (sorption sites of different strengths), with the adsorption energy increasing exponentially with the amount of adsorption sites. Furthermore, the interaction between dissolved molecules/adsorptive and non-uniform distribution of adsorption heat on the surface is also considered. Therefore, it can be assumed that the stronger sorption sites are occupied first, and the binding strength decreases as the sorption sites are occupied. Unlike the Langmuir isotherm, no q_{max} is defined here and is therefore more applicable to problems with low to medium concentrations [30–32]. The Langmuir sorption model, on the other hand, is based on the assumptions that adsorption occurs at energetically equivalent sorption sites, that the maximum amount of adsorbate (adsorptive bound to the adsorbents) cannot be higher than the available sorption sites (formation of a monolayer) and that there is no interaction between the dissolved molecules/adsorptive [32–34].

$$q = K_F \bullet {C_{eq}}^n \tag{4}$$

$$q = q_{max} \bullet \frac{K_L \bullet C_{eq}}{1 + K_L \bullet C_{eq}} \tag{5}$$

Since Freundlich and Langmuir are comparatively simple models, the calculations were extended to include a fixed bed model. Due to its simplicity, the BTCs were fitted with the Thomas model (shown in equation (6)).

$$\frac{C_{eq}}{C_0} = \frac{1}{1 + exp\left[\frac{K_{TH}}{Q} \bullet \left(q_{max} \bullet m - C_0 \bullet V_{Eff}\right)\right]} \tag{6}$$

In equation (6) K_{TH} [mL mg^{-1} min^{-1}] is the Thomas constant, m [g] the mass of adsorbent material inside the column and V_{Eff} [L] the effluent volume which has passed the column. The Thomas model is one of the most used models for representing the influence of adsorption parameters on the breakthrough of an analyte in a column system. It assumes reversible Langmuir kinetics of pseudo-second order, whereas axial dispersion is neglected [35–40].

3. Results and Discussion

3.1. Leaching of C-S-H phases

As the exact mass of the adsorbent is required, conducting leaching studies are essential as a first step for the data evaluation of the MCE. Fig. 2 shows the leached Ca(II)- and Si(IV)-concentrations of the four C-S-H phase leaching experiments (denoted as L1–L4 in Table 2) as well as the pH values. The results show that there is almost no relevant difference in the leaching behaviour between each experiment. With that it can be assumed that the ionic strength of the eluent (within the observed boundaries), the used filter disc and the injected medium show no influence on the leaching behaviour. It could therefore be shown that a reproducible leaching of the Circosil® is accomplished independent of the test parameters. The only variable that leads to a slight change in leaching behaviour is the pre-treatment (washing) of the Circosil®. When using the washed Circosil® (L2 and L3), comparatively more Ca (II) was leached in comparison to the untreated Circosil®. Considering the pH, the same pH of 10.7 was measured for all four experiments, which corresponds very well with the literature [23,26].

The literature also describes that systems of high initial C/S ratios (>1) preferably leach Ca(II). But when the C/S ratio decreased to approx. 0.8 the C-S-H phases dissolve congruently. On the other hand, C-S–H phases with C/S<0.8 preferably leach Si, again till they reach a C/S of 0.8 [26,27]. Assuming Circosil® has a C/S of approx. 0.65, the leached amounts of Ca(II) and Si(IV) (Fig. 2) fit the literature very well. Initially, significantly more Si(IV) (about 2.5 mmol/L) is released than Ca(II) (about 1 to 1.5 mmol/L), whereas later, equal amounts of Ca(II) and Si(IV) are released. The leaching behaviour of the washed Circosil® and the higher Ca(II) content leached also agrees very well with this observation. If, as already mentioned, more Si(IV) is initially leached at a C/S of about 0.65, the washing pre-treatment would increase the C/S. Accordingly, a higher Ca(II) concentration in the fractions would be expected in the leaching experiment. Irrespective of the slightly different Ca(II) concentrations in the fractions, the C/S in all fractions reach a value of approx. 1 after an eluent volume of 70 mL. The C/S in the remaining solids was not determined at this point but based on G. M. N. Baston et al. (2012) and A. W. Harris et al. (2002), a C/S in solution of 1 indicates a C/S in the solid of 0.8 due to the homogeneous dissolution of the C-S-H phase [22,26,27].

As mentioned, the exact mass of the adsorbents must be known for the calculations (see chapter 2.7), and any mass loss due to leaching must be considered. Furthermore, it has been shown that a reproducible leaching of Circosil® is ensured independent of the test parameters. Therefore, a simple model for the leaching could be developed. For each analyte measured the concentrations shown in Fig. 2 were averaged. Based on the averaged Ca(II) and Si(IV) concentrations, the corresponding leached oxygen concentrations were calculated using two different approaches: The first approach, shown in equation (7), is based on a tobermorite structure (cf. chapter 2.2) and for the second one, shown in equation (8), the oxygen concentration was calculated based on the precursors for C–S-H phases syntheses in laboratory scale; CaO and SiO_2 [41,42]. The n in equation (7) and (8) refers to the molar number of the elements.

$$n(O) = \frac{\left(\frac{17}{5} \bullet n(Ca) + \frac{17}{6} \bullet n(Si)\right)}{2} \tag{7}$$

$$n(O) = n(Ca) + 2 \bullet n(Si) \tag{8}$$

The results from equation (7) and (8) were averaged again. To determine the total mass loss, all averaged contents of O, Si, and Ca were then added. From this, the percentage loss could then be determined, plotted against the effluent volume and from this, by linear regression, the calculation basis for the mass loss depending on the effluent volume could be gained. The fit line of the linear regression is given as equation (9) ($R^2 = 0.996$).

$$massloss[\%] = 1.10154 + 0.0532 \bullet V_{Eff} \tag{9}$$

With equation (9), the Circosil® mass loss as a function of effluent volume can be considered in the Freundlich isotherm (Eq. (4)), Langmuir isotherm (Eq. (5)) and Thomas model (Eq. (6)). Doing so, those models rewrite as equation (10), (11) and (12):

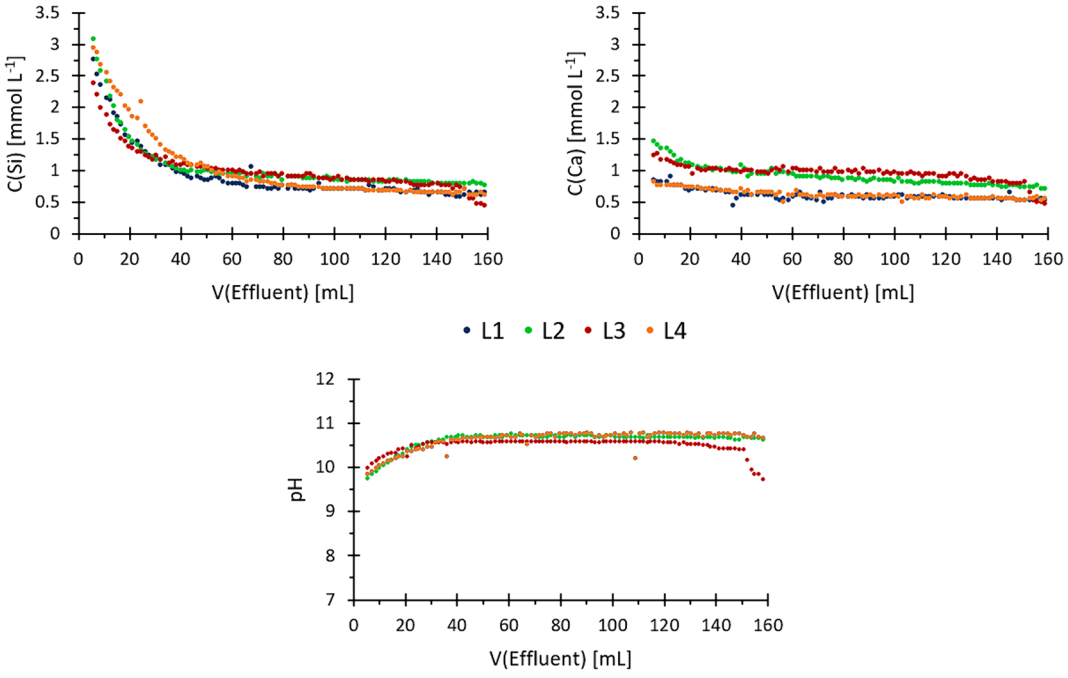

Fig. 2. Measured pH values, Ca and Si contents of the fractions in the individual leaching experiments (according to Table 2. L1 Circosil® in 10 mM NaCl, L2 washed Circosil® in 100 mM NaCl, L3 washed Circosil® in 10 mM NaCl, L4 Circosil® in 10 mM NaCl) plotted against the effluent volume.

$$q = \frac{m_{sorb}}{m_0 - \left(m_0\left(\frac{0.0532 \bullet V_{Eff} + 1.10154}{100}\right)\right)} = K_F \bullet {C_{eq}}^n \quad (10)$$

$$q = \frac{m_{sorb}}{m_0 - \left(m_0\left(\frac{0.0532 \bullet V_{Eff} + 1.10154}{100}\right)\right)} = q_{max} \bullet \frac{K_L \bullet C_{eq}}{1 + K_L \bullet C_{eq}} \quad (11)$$

$$\frac{C_{eq}}{C_0} = \frac{1}{1 + exp\left[\frac{K_{TH}}{Q} \bullet \left(q_{max} \bullet \left\{m_0 - \left(m_0\left(\frac{0.0532 \bullet V_{Eff} + 1.10154}{100}\right)\right)\right\} - C_0 \bullet V_{Eff}\right)\right]} \quad (12)$$

Where m_0 [g] is the initial weighed mass of adsorbent and m_{sorb} [mg] is the amount of analyte adsorbed on the solid.

3.2. Retention of Cs(I) on Circosil®

The retention of Cs(I) on Circosil® was investigated via MCE (with fraction collector) and via batch experiments. Fig. 3 shows the recovery (R) in [%] (BTC) and pH of MCE in 10 mM and 100 mM NaCl. Comparing the results for both eluents, a higher capacity of Cs(I) on Circosil® in 10 mM NaCl can be seen. This will be discussed in detail later. At this point it is also interesting to mention that here the same pH of 10.7 was reproducibly measured (analogue to the leaching study). As the measured Ca(II) and Si(IV) contents in the eluate are analogous to those in the leaching study, they are not listed and discussed again here.

Fig. 4 shows the Freundlich (Eq. (10)), Langmuir (Eq. (11)) and Thomas fits (Eq. (12)) of the data presented in Fig. 3. The Freundlich fits, with $R^2 = 0.939$ and 0.995, represent the experimental data way better than the Langmuir ones ($R^2 = 0.814$ and 0.970). With that it can be said that the MCEs are more likely based on Freundlich kinetics. Thus, and the theoretical principles described in chapter 2.7, a reversible sorption of Cs(I) to Circosil® in a kind of multilayer at heterogeneous sorption sites (of different binding strength) is most likely at this point. This observation agrees very well with the literature, where one to three different adsorption sites (ion exchange, outer-sphere and inner-sphere complexes) are proposed [13,43–46]. But also, according to the literature, the main sorption process of Cs(I) on cement paste phases is ion exchange on the C-S-H phases [4,47–50].

On the other hand, even though the Thomas model is mathematical based on kinetics analogous to Langmuir, both lead to different results [35,39,40]. Comparison of the correlation coefficients shows that the Thomas model ($R^2 = 0.992$ and 0.991) reflects reality much better than the Langmuir isotherm and at some point, even better than the Freundlich isotherm. This circumstance makes sense in so far as the Thomas model (along with Yoon-Nelson and Bohart-Adams) is precisely tailored to the fit of fixed-bed questions [51–54]. For this reason, the q_{max} values determined with the Thomas model are more reliable or reflect reality better than those calculated with the Langmuir isotherm. Another reason for the good Thomas fit could be due to the fact, that one dominant sorption process is assumed for the sorption of Cs(I) on C-S-H phases (see above). Thus, the kinetics is more like Freundlich, but has a noticeable Langmuir character due to the one dominant sorption process (homogeneous sorption sites). Nevertheless, the Thomas fits result in a q_{max} of 4.82 mg g^{-1} for Cs(I) on Circosil® in 10 mM NaCl and a q_{max} of 2.65 mg g^{-1} in 100 mM NaCl. Accordingly, a higher ionic strength of the electrolyte causes a drastic decrease of the Cs(I) capacity on C-S-H phases. A comparison of the Thomas constants (0.27 mL mg^{-1} min^{-1} in 10 mM NaCl and 0.31 mL mg^{-1} min^{-1} in 100 mM NaCl) supports these observations, thus a higher K_{TH} underlies faster saturation. This result is also in a very good agreement with literature. There is described that the ionic strength of the electrolyte and the competing ions (Na^+, K^+, and Ca^{2+}) are the main factors influencing Cs(I) sorption on C-S-H phases [55,56]. It should be mentioned that the C/S ratio of the C-S-H phases also strongly determines Cs(I) sorption. Thus, a higher C/S causes a lower Cs(I) adsorption and vice versa [48,56]. In the presented experiments, C/S was always the same, so that the influence can be neglected.

The sorption behaviour of Cs(I) on Circosil® could be described very well by means of MCE. However, since this is a completely new approach for column experiments, it is recommended to compare the results with those of an established experiment: batch experiments. For this reason, Fig. 5 shows the R_d values from the MCE and the batch plotted against C_{eq}.

Fig. 5 shows that the MCEs provide a significantly higher amount of data compared to the batch experiments. From the MCE-data, physicochemical parameters can be calculated more easily and, in case of doubt, more precisely. In the above case, the obtained data were fitted with simple exponential functions, the corresponding R_d values calculated for an C_{eq} of 15 mg/L Cs(I) and listed in Table 4. The value of C_{eq} was deliberately set to 15 mg/L since the column is saturated at this point and an equilibrium can be assumed.

The values in Table 4 show that the calculated log(R_d) values from MCE and batch are with a deviation of 2.0 % in 10 mM NaCl and 5.4 % in 100 mM NaCl close to each other. The influence of the ionic strength on the retention of Cs(I) on Circosil® can again been seen in both types of experiments. Since the Cs(I) sorption respectively the R_d values on C-S-H phases depend on the C/S ratio, the ionic strength of the electrolyte and also on the presence of competing ions, the values reported in the literature tend to vary greatly and a comparison is quite challenging [23,57]. A possible comparative value is provided by Missana et al. [56].

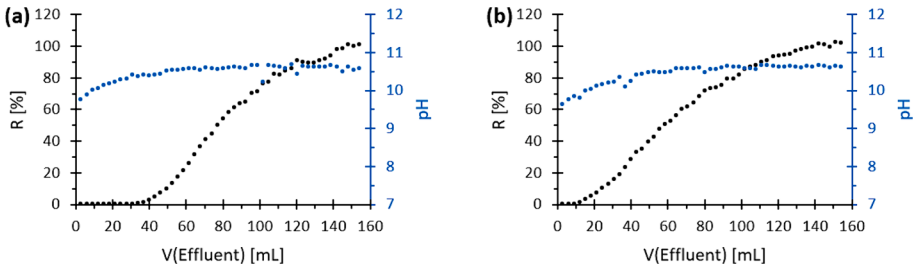

Fig. 3. Break through curve (BTC) of Cs(I) on Circosil® in [%] and pH plotted against the effluent volume for the MCEs: (a) in 10 mM (97.8 nmol Cs(I) per injection); (b) 100 mM NaCl (75.3 nmol Cs(I) per injection).

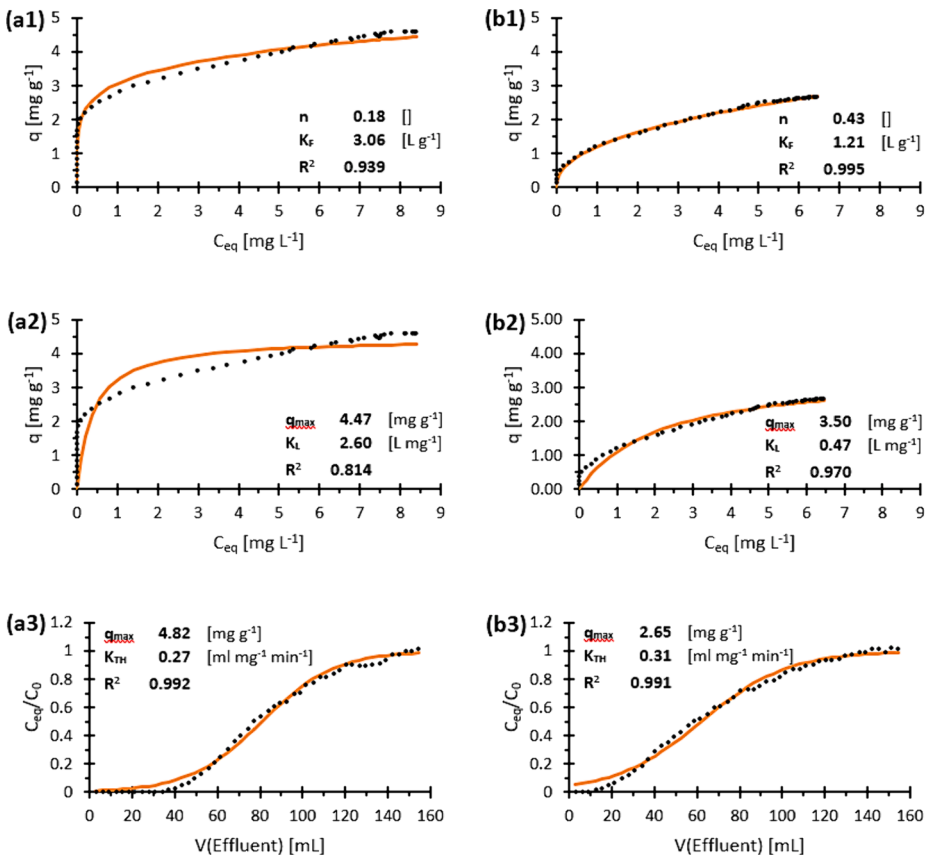

Fig. 4. Freundlich (1), Langmuir (2) and Thomas fit (3) for the MCEs with Cs(I) on Circosil® in 10 mM (a) and 100 mM NaCl (b).

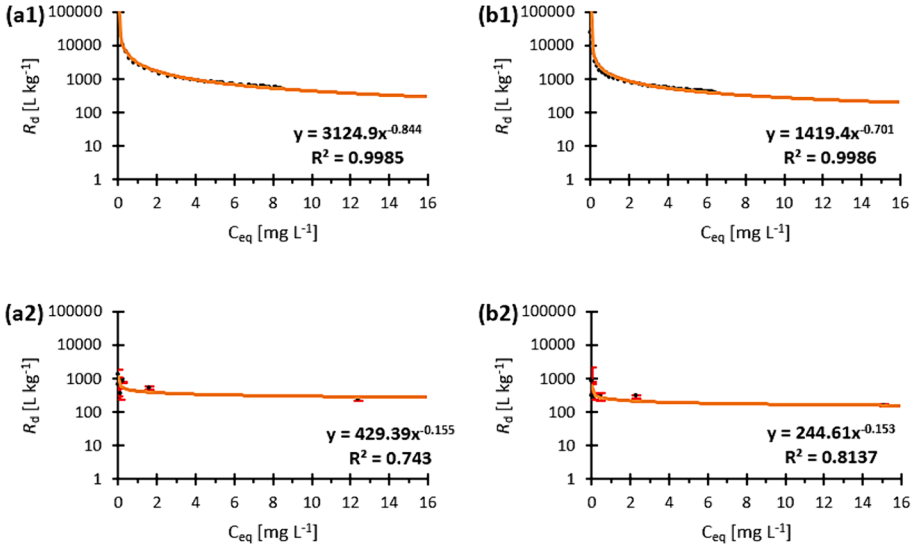

Fig. 5. R_d plotted against C_{eq} for Cs(I) in 10 mM NaCl (a) and 100 mM NaCl (b) obtained from MCE (1) and batch (2).

Table 4
Calculated R_d [L kg^{-1}] and log(R_d) values for miniaturised column experiments (MCE) and batch experiments.

R_d/log(R_d) [L kg^{-1}]	Cs(I) on Circosil® in **10 mM NaCl**	Cs(I) on Circosil® in **100 mM NaCl**
MCE	318/2.50	213/2.33
Batch	282/2.45	162/2.21

They had found an R_d (log(R_d)) of approximately 160 (2.20) L kg^{-1} for Cs(I) with quite similar experimental conditions, which is in a very good alignment with the gained values.

Finally, it should be mentioned that MCEs have a duration of 4 to 5 days according to the method described in chapter 2.3. Whereas for a comparable batch experiment approx. 2 to 3 weeks must be planned. Thus, significantly more data points can be generated via the MCE in a shorter period of time. Furthermore, dynamic instead of stationary sorption parameters can be calculated from this. Due to the almost identical R_d values, this circumstance is of secondary importance here, but in case of doubt it can reflect reality way better. In addition, similar sorption distribution ratios from stationary and dynamic experiments are a good hint of fast sorption kinetics.

3.3. Retention of Eu(III) on kaolinite/sand (MCE with HPLC-ICP-MS coupling)

The leaching behaviour of the 3:7 wt% kaolinite/sand mixture was investigated in advance analogously to Circosil®. However, there was no pronounced leaching (max. 38.9 µmol/L Al(III) and max. 23.6 µmol/LSi(IV) in solution), so it will not be discussed in detail.

Two experiments were performed with HPLC-ICP-MS coupling as described in chapter 2.6 (1:9 wt% kaolinite/sand and 100 % sand) and one without coupling as described in chapter 2.3 (3:7 wt% kaolinite/sand). Previous studies by Kautenburger et al. (2022) and Sander (2017) presented a first rudimentary approach for MCE-HPLC-ICP-MS setup. As this was not a robust method but a first draft, it was not possible to determine sorption parameters of any kind [8,10]. Thus, the sorption capacity of the analyte only could have been estimated. Even with the method presented in this paper, instrumental quantification of C_{eq} in the eluate is only possible with great effort. Due to the chosen experimental setup, however, an elegant assumption can now be made: To determine the sorption parameters for Eu(III) on kaolinite/sand, the fact that $C_{eq} = C_0$ or $C_0/C_{eq} = 1$ applies to the eluate when the column is saturated can be utilised. Thus, it is necessary to ensure column saturation and to normalise the BTC to the highest signals measured. Fig. 6 shows the chromatogram from the measurement with Eu(III) (6.6 nmol per Injection) at 1:9 wt% kaolinite/sand, the resulting Thomas fit and how it is achieved. Because of the large amount of the raw data, the chromatograms were first averaged for each injection. The averaged signals where than normalised to those of the internal standard (Ho) and fitted afterwards. Since the column was completely saturated, it is assumed for the fit, as described above, that the following applies for the largest normalised signal: $C_0/C_{eq} = 1$.

Table 5
Fit Parameters for Eu(III) on different kaolinite/sand mixtures in 10 mM NaCl.

Ratio		Fit Parameters		
Kaolinite	Sand	q_{max} [mg g^{-1}]	K_{TH} [mL mg^{-1} min^{-1}]	R^2
0	10	0.09	224.7	0.996
1	9	0.12	63.9	0.997
3	7	0.22	1.43	0.983

The dip in the chromatogram shown in Fig. 6 (1) is due to a small error in the measurement setup, which is well documented and did not distort the experiment in any way. Nevertheless, the affected data points are excluded for further consideration (see Fig. 6 (2) and (3)). Again, the Thomas model provides an excellent fit to the measured data with a $R^2 = 0.997$. This results in a q_{max} of 0.12 mg g^{-1} and a Thomas constant of 63.9 mL mg^{-1} min^{-1} for Eu(III) at the 1:9 wt% kaolinite/sand mixture in 10 mM NaCl. The same procedure (shown in Fig. 6) was also applied to the measured data for Eu(III) on 100 % sand in 10 mM NaCl, whereas the data for Eu(III) on 3:7 wt% kaolinite/sand where evaluated as shown in Fig. 4 (since the experiment was performed analogously to the MCE with Cs(I) Circosil®). For a better comparison, the fit parameters for all Eu (III) experiments are listed in Table 5.

As can be seen from Table 5, a lower kaolinite content results in a lower q_{max} and a higher K_{TH}. Accordingly, the absorptive capacity of kaolinite towards Eu(III) must be significantly higher than that of sand. If the q_{max} values from Table 5 are now plotted against the kaolinite content used, it is possible to calculate the q_{max} for Eu(III) at 100 % kaolinite by linear extrapolation. The fit line of this linear regression is given as equation (13) ($R^2 = 0.988$).

$$q_{max} = 0.084 + 0.0044 \bullet (\textit{fraction of kaolinite}\ [\%]) \quad (13)$$

With that a q_{max} of 0.52 mg g^{-1} can be calculated for Eu(III) on kaolinite in 10 mM NaCl and the corresponding value for sand (0 % kaolinite) can be seen in Table 5 (q_{max} = 0.09 mg g^{-1}). As comparison, Kautenburger and Beck (2010) had found a q_{max} of 0.47 mg g^{-1} for Eu(III) on kaolinite in 10 mM $NaClO_4$ using batch experiments at similar conditions [58].

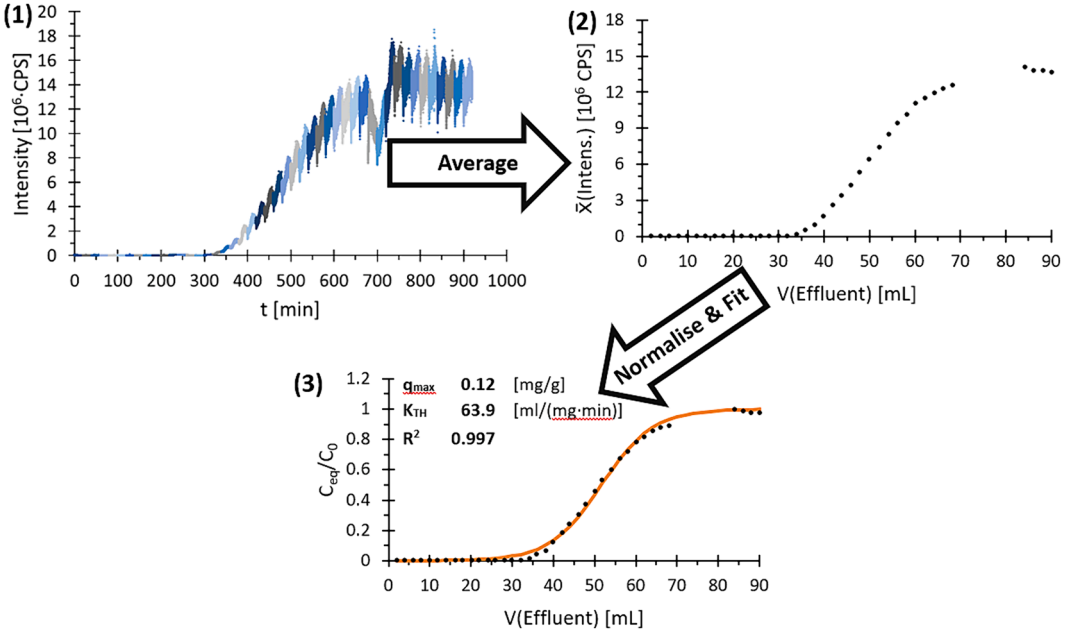

Fig. 6. Chromatogram (1) averaged signals for each injection (2) and resulting Thomas fit (3) for Eu(III) on 1:9 wt% kaolinite/sand in 10 mM NaCl.

Where on the other hand Qiu et al. (2019) had found an identical q_{max} of 0.09 mg g^{-1} for Eu(III) on sand [59]. The values for Eu(III) on sand fit excellently, while the ones obtained for Eu(III) on kaolinite deviates by 11 % from the literature. The reason for this small discrepancy can either be due to the normal uncertainty range or a slight overdetermination of q_{max} for Eu(III) on the 3:7 wt% kaolinite/sand mixture. The linear regression of the q_{max} values had shown that this one value is slightly above the fitted line. In addition, the coefficient of determination for this data point (0.983, cf. Table 5) is lower than that of the other two values, which could indicate a slight uncertainty of the value.

In the end it was proven that with HPLC-ICP-MS coupling MCEs can be carried out in just a few hours without additional treatment needed. With that the advantage of saving time defined at the end of chapter 3.2 weighs even more. However, there is also a small limitation here; due to the direct introduction of the eluate into the ICP-MS, the ionic strength of the eluate must be within the limits defined by the manufacturer. Consequently, coupling using Circosil® as adsorbent is not possible. But for most sorbents, the direct coupling method and data evaluation presented here can be used to determine realistic sorption data very fast.

4. Conclusion

In this study, a new method for fast and dynamic sorption experiments using HPLC, ICP-MS and HPLC-ICP-MS coupling, including a new approach for data evaluation, is presented.

With the MCE-method a maximum loading capacity of 4.82 mg g^{-1} in 10 mM NaCl and 2.65 mg g^{-1} in 100 mM NaCl was determined for Cs(I) on Circosil®. Maximum loading capacities are also achievable by batch but only with greater effort and not with this reliability. Therefore, for a MCE-batch-comparison, the obtained log(R_d) values were compared. With log(R_d) of 2.50/2.45 L kg^{-1} (MCE/batch) in 10 mM NaCl and 2.33/2.21 L kg^{-1} in 100 mM NaCl, those differed only by 2.0 % and 5.4 % and where also in a good alignment with literature. Accordingly, it was shown that MCEs can not only be used to determine more sorption parameters, but also much faster and, due to the significantly higher data density, more accurately than with a conventional batch method.

Apart from sorption experiments, another possible application for MCE was presented. In the context of C-S-H phases, the same experimental setup was used to perform a leaching study on Circosil®. A reproducible leaching behaviour of Circosil® was demonstrated, which again is in excellent agreement with the literature. From this, a simple model for predicting the mass loss of Circosil® in the column as a function of the eluent volume could be derived.

In addition, the MCE method has been further developed to implement an even faster online quantification via direct HPLC-ICP-MS coupling. Thus, a maximum loading capacity of 0.52 mg g^{-1} was determined for Eu(III) on kaolinite in 10 mM NaCl and 0.09 mg g^{-1} on sand. Those results are again in a very good alignment with the literature.

In summary, this study presented a new experimental method (including data evaluation) for performing fast and dynamic sorption and leaching experiments by means of MCEs. Dynamic retention coefficients and maximum loading capacities for two different analytes on several adsorbent materials could be determined easily and very accurately. The method presented works much faster, with less resources and more controllable than the conventional experimental setups. In this context, controllable means, that the pressure, temperature, flow and gradient of the eluent can be precisely monitored and adjusted. In addition, the MCE method should also be easily applicable to a wider range of analytes and adsorbent materials; something that will be investigated in the future.

CRediT authorship contribution statement

Aaron Haben: Writing – original draft, Visualization, Validation, Methodology, Investigation, Formal analysis, Data curation, Conceptualization. **Kristina Brix:** Writing – review & editing, Validation. **Nico Bachmann:** Visualization, Investigation. **Ralf Kautenburger:** Writing – review & editing, Supervision, Project administration, Funding acquisition, Conceptualization.

Declaration of competing interest

The authors declare that they have no known competing financial interests or personal relationships that could have appeared to influence the work reported in this paper.

Data availability

Data will be made available on request.

Acknowledgements

This work was supported by the German Federal Ministry for the Environment, Nature Conservation, Nuclear Safety and Consumer Protection (BMUV), represented by the Project Management Agency Karlsruhe (PTKA-WTE) [grant number 02E11860D]. ICP-QQQ instrumentation for this work was financially supported from Saarland University and German Research Foundation [project number INST 256/553-1]. We would like to thank our project partners for the kind collaboration and Anna Jennewein for the assistance with the Graphical Abstract.

References

[1] R. Kautenburger, H.P. Beck, Waste disposal in clay formations: influence of humic acid on the migration of heavy-metal pollutants, ChemSusChem 1 (2008) 295–297, https://doi.org/10.1002/cssc.200800014.
[2] R. Hahn, C. Hein, J.M. Sander, R. Kautenburger, Complexation of europium and uranium with natural organic matter (NOM) in highly saline water matrices analysed by ultrafiltration and inductively coupled plasma mass spectrometry (ICP-MS), Appl. Geochem. 78 (2017) 241–249, https://doi.org/10.1016/j.apgeochem.2017.01.008.
[3] C. Hein, J.M. Sander, R. Kautenburger, New approach of a transient ICP-MS measurement method for samples with high salinity, Talanta 164 (2017) 477–482, https://doi.org/10.1016/j.talanta.2016.06.059.
[4] S. Baur, K. Brix, A. Feuerstein, O. Janka, R. Kautenburger, Retention of waste cocktail elements onto characterised calcium silicate hydrate (C–S–H) phases: A kinetic study under highly saline and hyperalkaline conditions, Appl. Geochem. 143 (2022) 105319, https://doi.org/10.1016/j.apgeochem.2022.105319.
[5] K. Brix, S. Baur, A. Haben, R. Kautenburger, Building the bridge between U(VI) and Ca-bentonite – Influence of concentration, ionic strength, pH, clay composition and competing ions, Chemosphere 285 (2021) 131445, https://doi.org/10.1016/j.chemosphere.2021.131445.
[6] K. Brix, C. Hein, A. Haben, R. Kautenburger, Adsorption of caesium on raw Ca-bentonite in high saline solutions: Influence of concentration, mineral composition, other radionuclides and modelling, Appl. Clay Sci. 182 (2019) 105275, https://doi.org/10.1016/j.clay.2019.105275.
[7] T.-H. Wang, M.-H. Li, S.-P. Teng, Bridging the gap between batch and column experiments: A case study of Cs adsorption on granite, J. Hazard. Mater. 161 (2009) 409–415, https://doi.org/10.1016/j.jhazmat.2008.03.112.
[8] R. Kautenburger, K. Brix, S. Baur, J.M. Sander, Development of mini column experiments (MCE) by coupling microliter flow HPLC with ICP-MS for the analysis of metal retention under conditions close to nature, Talanta Open 5 (2022), https://doi.org/10.1016/j.talo.2022.100111.
[9] R. Kautenburger, A new timescale dimension for migration experiments in clay: proof of principle for the application of miniaturized clay column experiments (MCCE), J. Radioanal. Nucl. Chem. 300 (2014) 255–262, https://doi.org/10.1007/s10967-014-3017-1.
[10] J. Sander, Entwicklung von Methoden zur Untersuchung der Metallmobilität an Ton in Salinaren Systemen, Anorganische Festkörperchemie/Elementanalytik, Universität des Saarlandes, Saarbrücken (2017), https://doi.org/10.22028/D291-26994.
[11] N. Hakem, I. Al Mahamid, J. Apps, G. Moridis, Sorption of Cesium and Strontium on Hanford Soil, J. Radioanal. Nucl. Chem. 246 (2000) 275–278, https://doi.org/10.1023/a:1006701902891.
[12] L. Dzene, E. Tertre, F. Hubert, E. Ferrage, Nature of the sites involved in the process of cesium desorption from vermiculite, J. Colloid Interface Sci. 455 (2015) 254–260, https://doi.org/10.1016/j.jcis.2015.05.053.
[13] K. Brix, A. Haben, R. Kautenburger, Time-Dependent Retention of a Mixture of Cs (I), Sm(III), Eu(III) and U(VI) as Waste Cocktail by Calcium Silicate Hydrate (C-S-H) Phases, Minerals 13 (2023) 1469, https://doi.org/10.3390/min13121469.

[14] M. Eisenbud, K. Krauskopf, E.P. Franca, W. Lei, R. Ballad, P. Linsalata, K. Fujimori, Natural analogues for the transuranic actinide elements: An investigation in Minas Gerais, Brazil, Environmental Geology and Water Sciences 6 (1984) 1–9, https://doi.org/10.1007/BF02525564.

[15] K.B. Krauskopf, Thorium and rare-earth metals as analogs for actinide elements, Chemical Geology 55 (1986) 323–335, https://doi.org/10.1016/0009-2541(86)90033-1.

[16] J. Tits, T. Stumpf, T. Rabung, E. Wieland, T. Fanghänel, Uptake of Cm(III) and Eu (III) by Calcium Silicate Hydrates: A Solution Chemistry and Time-Resolved Laser Fluorescence Spectroscopy Study, Environmental Science & Technology 37 (2003) 3568–3573, https://doi.org/10.1021/es030020b.

[17] M. Jobmann, A. Bebiolka, V. Burlaka, P. Herold, S. Jahn, A. Lommerzheim, J. Maßmann, A. Meleshyn, S. Mrugalla, K. Reinhold, A. Rübel, L. Stark, G. Ziefle, Safety assessment methodology for a German high-level waste repository in clay formations, J. Rock Mech. Geotech. Eng. 9 (2017) 856–876, https://doi.org/10.1016/j.jrmge.2017.05.007.

[18] M.V. Dingankar, V. Kalyanasundaram, M. Srinivasan, A reassessment of long-lived actinide waste hazard potential from Th-223U-fueled reactors, Waste Manage. 12 (1992) 359–372, https://doi.org/10.1016/0956-053X(92)90039-L.

[19] H. Freiesleben, Final disposal of radioactive waste, EPJ Web Conf. 54 (2013), https://doi.org/10.1051/epjconf/20135401006.

[20] A. Lommerzheim, M. Jobmann, A. Meleshyn, S. Mrugalla, A. Rübel, L. Stark, Safety concept, FEP catalogue and scenario development as fundamentals of a long-term safety demonstration for high-level waste repositories in German clay formations, Geological Society Special Publication 482 (2019) 313–329, https://doi.org/10.1144/SP482.6.

[21] B. Zlobenko, Y. Fedorenko, Y. Olkhovyk, S. Buhera, A. Rozko, Test of the Thermal-Hydro-mechanical Behaviors of Cherkasy Bentonite as Buffer Material of HLW Repository, in: A. Zaporozhets, O. Popov (Eds.) Systems, Decision and Control in Energy IV: Volume II. Nuclear and Environmental Safety, Springer Nature Switzerland, Cham, 2023, pp. 185-196, doi: 10.1007/978-3-031-22500-0_12.

[22] X. Gaona, R. Dähn, J. Tits, A.C. Scheinost, E. Wieland, Uptake of Np(IV) by C-S–H Phases and Cement Paste: An EXAFS Study, Environ. Sci. Technol. 45 (2011) 8765–8771, https://doi.org/10.1021/es2012897.

[23] M. Ochs, D. Mallants, L. Wang, Radionuclide and metal sorption on cement and concrete, Springer, 2016, doi: 10.1007/978-3-319-23651-3.

[24] R.D. Spence, Chemistry and microstructure of solidified waste forms, Lewis Publishers, Boca Raton, 1993.

[25] E. Reinoso-Maset, J. Ly, Study of Major Ions Sorption Equilibria To Characterize the Ion Exchange Properties of Kaolinite, J. Chem. Eng. Data 59 (2014) 4000–4009, https://doi.org/10.1021/je5005438.

[26] G.M.N. Baston, A.P. Clacher, T.G. Heath, F.M.I. Hunter, V. Smith, S.W. Swanton, Calcium silicate hydrate (C-S-H) gel dissolution and pH buffering in a cementitious near field, Mineral. Mag. 76 (2012) 3045–3053, https://doi.org/10.1180/minmag.2012.076.8.20.

[27] A.W. Harris, M.C. Manning, W.M. Tearle, C.J. Tweed, Testing of models of the dissolution of cements—leaching of synthetic CSH gels, Cem. Concr. Res. 32 (2002) 731–746, https://doi.org/10.1016/S0008-8846(01)00748-7.

[28] Circosil® an Overview, Datasheet, Cirkel GmbH & Co. KG, 2021.

[29] Circosil® - Chemical composition, Datasheet, Cirkel GmbH & Co. KG, 2021.

[30] H. Freundlich, Über die Adsorption in Lösungen, Z. Phys. Chem. 57 (1907) 385–470, https://doi.org/10.1515/zpch-1907-5723.

[31] K. Vijayaraghavan, T.V.N. Padmesh, K. Palanivelu, M. Velan, Biosorption of nickel (II) ions onto Sargassum wightii: Application of two-parameter and three-parameter isotherm models, J. Hazard. Mater. 133 (2006) 304–308, https://doi.org/10.1016/j.jhazmat.2005.10.016.

[32] M. Ghaedi, Adsorption: Fundamental processes and applications, Interface Science and Technology, Elsevier (2021) 2–713, https://doi.org/10.1016/c2018-0-02771-1.

[33] I. Langmuir, The adsorption of gases on plane surfaces made of glass, mica and platinum, J. Am. Chem. Soc. 40 (1918) 1361–1403, https://doi.org/10.1021/ja02242a004.

[34] R.H. Fowler, A Statistical Derivation of Langmuir's Adsorption Isotherm, Math. Proc. Cambridge 31 (1935) 260–264, https://doi.org/10.1017/S0305004100013359.

[35] H.C. Thomas, Chromatography: A problem in kinetics, Ann. N.Y. Acad. Sci. 49 (1948) 161–182, https://doi.org/10.1111/j.1749-6632.1948.tb35248.x.

[36] K.H. Chu, Breakthrough curve analysis by simplistic models of fixed bed adsorption: In defense of the century-old Bohart-Adams model, Chem. Eng. J. 380 (2020) 122513, https://doi.org/10.1016/j.cej.2019.122513.

[37] G. Yan, T. Viraraghavan, M. Chen, A New Model for Heavy Metal Removal in a Biosorption Column, Adsorp. Sci. Technol. 19 (2001) 25–43, https://doi.org/10.1260/0263617011493953.

[38] E.I. Unuabonah, B.I. Olu-Owolabi, E.I. Fasuyi, K.O. Adebowale, Modeling of fixed-bed column studies for the adsorption of cadmium onto novel polymer–clay composite adsorbent, J. Hazard. Mater. 179 (2010) 415–423, https://doi.org/10.1016/j.jhazmat.2010.03.020.

[39] C. Tien, Introduction to Adsorption: Basics, Analysis, and Applications, Elsevier, Amsterdam, 2019, doi: 10.1016/C2018-0-00297-2.

[40] H.C. Thomas, Heterogeneous Ion Exchange in a Flowing System, J. Am. Chem. Soc. 66 (1944) 1664–1666, https://doi.org/10.1021/ja01238a017.

[41] M. Atkins, F.P. Glasser, A. Kindness, Cement hydrate phase: Solubility at 25°C, Cem. Concr. Res. 22 (1992) 241–246, https://doi.org/10.1016/0008-8846(92)90062-Z.

[42] J. Tits, E. Wieland, C.J. Müller, C. Landesman, M.H. Bradbury, Strontium binding by calcium silicate hydrates, J. Colloid Interface Sci. 300 (2006) 78–87, https://doi.org/10.1016/j.jcis.2006.03.043.

[43] E. Duque-Redondo, Y. Kazuo, I. López-Arbeloa, H. Manzano, Cs-137 immobilization in C-S-H gel nanopores, Phys. Chem. Chem. Phys. 20 (2018) 9289–9297, https://doi.org/10.1039/C8CP00654G.

[44] T.G. Heath, D.J. Ilett, C.J. Tweed, Thermodynamic Modelling of the Sorption of Radioelements onto Cementitious Materials, MRS Online Proc. Library 412 (1995) 443, https://doi.org/10.1557/PROC-412-443.

[45] J. Jiang, P. Wang, D. Hou, The mechanism of cesium ions immobilization in the nanometer channel of calcium silicate hydrate: a molecular dynamics study, Phys. Chem. Chem. Phys. 19 (2017) 27974–27986, https://doi.org/10.1039/C7CP05437H.

[46] T. Missana, M. García-Gutiérrez, M. Mingarro, U. Alonso, Analysis of barium retention mechanisms on calcium silicate hydrate phases, Cem. Concr. Res. 93 (2017) 8–16, https://doi.org/10.1016/j.cemconres.2016.12.004.

[47] S. Aggarwal, M. Angus, J. Ketchen, Sorption of radionuclides onto specific mineral phases present in repository cements, AEA Technology, 2000. Report NSS/R312,.

[48] M. Ochs, I. Pointeau, E. Giffaut, Caesium sorption by hydrated cement as a function of degradation state: Experiments and modelling, Waste Manage. 26 (2006) 725–732, https://doi.org/10.1016/j.wasman.2006.01.033.

[49] B. Allard, Mechanisms for the Interaction of Americium(III) and Neptunium(V) with Geologic Media, MRS Online Proc. Library 26 (1983) 899, https://doi.org/10.1557/PROC-26-899.

[50] K. Andersson, B. Allard, B. Torstenfelt, Sorption and diffusion studies of Cs and I in concrete, SKBF/KBS TR 83-13, Swedish Nuclear Fuel Supply Company, 1983.

[51] K.L. Tan, B.H. Hameed, Insight into the adsorption kinetics models for the removal of contaminants from aqueous solutions, J. Taiwan Inst. Chem. E 74 (2017) 25–48, https://doi.org/10.1016/j.jtice.2017.01.024.

[52] R. Apiratikul, K.H. Chu, Improved fixed bed models for correlating asymmetric adsorption breakthrough curves, J. Water Process Eng. 40 (2021) 101810, https://doi.org/10.1016/j.jwpe.2020.101810.

[53] Y.H. Yoon, J.H. Nelson, Application of Gas Adsorption Kinetics I. A Theoretical Model for Respirator Cartridge Service Life, Am. Ind. Hyg. Assoc. J. 45 (1984) 509–516, https://doi.org/10.1080/15298668491400197.

[54] G.S. Bohart, E.Q. Adams, Some aspects of the behavior of charcoal with respect to chlorine, J. Am. Chem. Soc. 42 (1920) 523–544, https://doi.org/10.1021/ja01448a018.

[55] S. Höglund, L. Eliasson, B. Allard, K. Andersson, B. Torstenfelt, Sorption of Some Fission Products and Actinides in Concrete Systems, MRS Online Proc. Library 50 (1985) 683, https://doi.org/10.1557/PROC-50-683.

[56] T. Missana, M. García-Gutiérrez, M. Mingarro, U. Alonso, Comparison between cesium and sodium retention on calcium silicate hydrate (CSH) phases, Appl. Geochem. 98 (2018) 36–44, https://doi.org/10.1016/j.apgeochem.2018.09.007.

[57] I. Pointeau, N. Marmier, F. Fromage, M. Fedoroff, E. Giffaut, Cesium and Lead Uptake by CSH Phases of Hydrated Cement, MRS Online Proc. Library 663 (2000) 97, https://doi.org/10.1557/PROC-663-97a.

[58] R. Kautenburger, H.P. Beck, Influence of geochemical parameters on the sorption and desorption behaviour of europium and gadolinium onto kaolinite, J. Environ. Monit. 12 (2010) 1295–1301, https://doi.org/10.1039/B914861B.

[59] L. Qiu, K. Scott, S. Rousseau, Kinetic and equilibrium studies of Cs(I), Sr(II) and Eu (III) adsorption on a natural sandy soil, Radiochim. Acta 107 (2019) 55–66, https://doi.org/10.1515/ract-2018-2976.